Biochemical and Biophysical Research Communications 440 (2013) 594–598

Contents lists available at ScienceDirect

Biochemical and Biophysical Research Communications

journal homepage: www.elsevier.com/locate/ybbrc

Extra-structural elements in the RNA recognition motif in archaeal Pop5 play a crucial role in the activation of RNase P RNA from *Pyrococcus horikoshii* OT3

Kohsuke Hazeyama [a], Masato Ishihara [b], Toshifumi Ueda [b], Etsuko Nishimoto [c], Takashi Nakashima [a,b], Yoshimitsu Kakuta [a,b], Makoto Kimura [a,b,*]

[a] *Laboratory of Biochemistry, Department of Bioscience and Biotechnology, Graduate School, Faculty of Agriculture, Kyushu University, Hakozaki 6-10-1, Higashi-ku, Fukuoka 812-8581, Japan*
[b] *Laboratory of Structural Biology, Graduate School of Systems Life Sciences, Kyushu University, Hakozaki 6-10-1, Fukuoka 812-8581, Japan*
[c] *Institute of Biophysics, Department of Bioscience and Biotechnology, Graduate School, Faculty of Agriculture, Kyushu University, Hakozaki 6-10-1, Fukuoka 812-8581, Japan*

ARTICLE INFO

Article history:
Received 15 September 2013
Available online 10 October 2013

Keywords:
Archaea
Pyrococcus horikoshii
Protein–RNA interaction
RNA chaperone
RNA recognition motif

ABSTRACT

Ribonuclease P (RNase P) is a ribonucleoprotein complex essential for the processing of 5′ leader sequences of precursor tRNAs (pre-tRNA). *Pho*Pop5 is an archaeal homolog of human RNase P protein hPop5 involved in the activation of RNase P RNA (*Pho*pRNA) in the hyperthermophilic archaeon *Pyrococcus horikoshii*, probably by promoting RNA annealing (AN) and RNA strand displacement (SD). Although *Pho*Pop5 folds into the RNA recognition motif (RRM), it is distinct from the typical RRM in that it has an insertion of α-helix (α2) between α1 and β2. Biochemical and structural data have shown that the dimerization of *Pho*Pop5 through the loop between α1 and α2 is required for the activation of *Pho*pRNA. In addition, *Pho*Pop5 has additional helices (α4 and α5) at the C-terminus, which pack against one face of the β-sheet. In this study, we examined the contribution of the C-terminal helices to the activation of *Pho*pRNA using mutation analyses. Reconstitution experiments and fluorescence resonance energy transfer (FRET)-based assays indicated that deletion of the C-terminal helices α4 and α5 significantly influenced on the pre-tRNA cleavage activity and abolished AN and SD activities, while that of α5 had little effect on these activities. Moreover, the FRET assay showed that deletion of the loop between α1 and α2 had no influence on the AN and SD activity. Further mutational analyses suggested that basic residues at α4 are involved in interaction with *Pho*pRNA, while hydrophobic residues at α4 participate in interaction with hydrophobic residues at the β-sheet, thereby stabilizing an appropriate orientation of the helix α4. Together, these results indicate that extra-structural elements in the RRM in *Pho*Pop5 play a crucial role in the activation of *Pho*pRNA.

1. Introduction

Ribonuclease P (RNase P) is a ribonucleoprotein (RNP) that catalyzes the processing of 5′ leader sequences from tRNA precursors (pre-tRNA) and other noncoding RNAs in all living cells [1,2]. Although the functionality of RNase P remains almost the same from bacteria to humans, the chemical composition of this enzyme differs in the three phylogenetic domains of life. Eubacterial RNase P is composed of a catalytic RNA and a single protein subunit, and in the presence of a high concentration of Mg^{2+}, the eubacterial RNase P RNA itself can hydrolyze pre-tRNA *in vitro* [3]. In contrast, archaeal and eukaryotic RNase Ps comprise a single RNA moiety and multiple proteins: 4 or 5 for archaeal RNase Ps and as many as 10 for eukaryotic RNase Ps [4]. Although the RNA components in archaea and eukaryotes alone have little catalytic activity *in vitro* [5,6], they function in cooperation with protein subunits in substrate recognition and catalysis. Hence, archaeal and eukaryotic RNase Ps may serve as a model RNP for studying how a functional RNA can be activated by protein cofactors and how the RNP enzymes catalyze biological processes.

We earlier found that RNase P RNA (*Pho*pRNA) and five proteins in the hyperthermophilic archaeon *Pyrococcus horikoshii* OT3 reconstituted RNase P activity that exhibits enzymatic properties like those of the authentic enzyme [7,8]. The *P. horikoshii* RNase P proteins were designated *Pho*Pop5, *Pho*Rpp38, *Pho*Rpp21,

Abbreviations: AN, RNA annealing; CD, circular dichroism; FRET, fluorescence resonance energy transfer; *Pho*pRNA, ribonuclease P RNA from *P. horikoshii*; RNase P, ribonuclease P; pre-tRNA, precursor tRNA; SD, strand displacement.

* Corresponding author at: Laboratory of Biochemistry, Department of Bioscience and Biotechnology, Graduate School, Faculty of Agriculture, Kyushu University, Hakozaki 6-10-1, Higashi-ku, Fukuoka 812-8581, Japan. Fax: +81 92 642 2853.
E-mail address: mkimura@agr.kyushu-u.ac.jp (M. Kimura).

0006-291X/$ - see front matter © 2013 Elsevier Inc. All rights reserved.
http://dx.doi.org/10.1016/j.bbrc.2013.09.140

*Pho*Rpp29, and *Pho*Rpp30, according to their sequence homology with the human RNase P proteins hPop5, Rpp21, Rpp29, Rpp30, and Rpp38, respectively [9]. Biochemical and structural studies revealed that *Pho*Pop5 and *Pho*Rpp21 form a complex with *Pho*Rpp30 and *Pho*Rpp29, and the resulting complexes, *Pho*Pop5-*Pho*Rpp30 and *Pho*Rpp21-*Pho*Rpp29, are involved in activation of the C- and S-domains, respectively [10–12]. Recently, fluorescence resonance energy transfer (FRET)-based assays indicated that *Pho*Pop5, *Pho*Rpp21, *Pho*Rpp29, and *Pho*Rpp30 can promote RNA annealing (AN) and strand displacement (SD), while *Pho*Rpp38 has no influence on FRET [13]. Hence, the four proteins may assist *Pho*pRNA in attaining a functionally active conformation by promoting AN and SD.

*Pho*Pop5 consists of a five-stranded antiparallel β-sheet and five helices, which fold in a way that is topologically similar to the RNA recognition motif (RRM) [10]. *Pho*Pop5 is, however, distinct from the typical RRM in that it has an insertion of α-helix (α2) between α1 and β2. In addition, it has additional helices (α4 and α5) at the C-terminus, which pack against one face of the β-sheet and form an electropositive patch suitable for RNA binding [10]. It was previously shown that Glu44 and Glu48 at the loop between α1 and α2 are involved in the dimerization of *Pho*Pop5, and that this dimerization is required for the pre-tRNA cleavage activity [10]. In this study, to evaluate the involvement of the C-terminal extension in the functional activity of *Pho*Pop5, we prepared two mutants, Δ6C and Δ14C, in which the 6 and 14 C-terminal amino acids were deleted, respectively, and characterized them with respect to pre-tRNA cleavage activity and to the promoting activity of AN and SD. Truncation of 14 residues significantly reduced the pre-tRNA cleavage activity and abolished both AN and SD activities, while that of 6 residues had little effect on these activities. Moreover, it was found that deletion of the loop between α1 and α2 had no influence of FRET efficiency. Further mutational analyses indicated that positively charged residues, Lys108 and Lys112, at α4 are fully involved in interaction with *Pho*pRNA, while hydrophobic residues, such as Phe113 and Leu114, are involved in hydrophobic interaction with the β-sheet, thereby stabilizing an appropriate orientation of the helix α4. The present study shows that extra-structural elements in the RRM in *Pho*Pop5 play a crucial role in the activation of *Pho*pRNA; that is, the C-terminal extension in the dimerized *Pho*Pop5 through the loop between α1 and α2 is essential for the activation of *Pho*pRNA by promoting AN and SD.

2. Materials and methods

2.1. Materials

Five RNase P proteins (*Pho*Pop5, *Pho*Rpp21, *Pho*Rpp29, *Pho*Rpp30, and *Pho*Rpp38), *Pho*pRNA, and pre-tRNA^{Tyr} in *P. horikoshii* were prepared as described previously [7,8]. The deletion mutant ΔL43–48, in which the residues 43–48 including Glu44 and Glu48 were deleted, was prepared as described previously [10]. Restriction enzymes were purchased from MBI Fermentas (Ontario, Canada). Oligonucleotides were purchased from Sigma–Aldrich (St. Louis, MO). Two fluorescence-labeled synthetic oligoribonucleotides (Cy3-21R− and Cy5-21R+) were purchased from Operon Biotechnologies (Tokyo, Japan). Ex Taq DNA polymerase and the DNA ligation kit were purchased from Takara Bio (Shiga, Japan). All other chemicals were of analytical grade for biochemical use.

2.2. Preparation of mutant proteins

Deleted mutations and site-directed mutagenesis were produced by oligonucleotide-based mutagenesis. Mutations were identified by DNA sequence determination; the entire sequence of each mutant gene was determined to rule out that any additional mutations had arisen during the mutagenesis reaction steps. The resulting mutants were purified using the same protocol as used for the wild-type *Pho*Pop5 [10].

2.3. Far-ultraviolet circular dichroism (CD)

CD spectra in the far-ultraviolet range, 200–250 nm, were recorded at room temperature on a Jasco J-720 spectropolarimeter. Proteins were dissolved to a final concentration of 100 μg/mL in 50 mM Tris–HCl, pH 7.5, containing 200 mM NaCl. Signal averaging during the accumulation of four scans was done automatically.

2.4. Assay for pre-tRNA cleavage activity

The RNase P activity for the reconstituted particles containing *Pho*Pop5 or its mutants was analyzed, principally as described previously [14]. The reaction mixtures were incubated in the reconstitution buffer, 50 mM Tris–HCl (pH 7.6) containing 50 mM $MgCl_2$, 600 mM NH_4OAc, 60 mM NH_4Cl, *Pho*pRNA or its mutants (20 pmol), the five proteins (each 20 pmol), and pre-tRNA^{Tyr} (2.5 μg), at 75 °C for specified periods. The reactions were stopped by adding phenol, and the reaction products were separated on 10% polyacrylamide denaturing gels in TBE buffer (900 mM Tris–borate containing 10 mM EDTA) at 150 V for 1 h. After electrophoresis, the reaction products were visualized by staining in a 0.1% toluidine blue solution. The resulting image was used to obtain values for the pre-tRNA^{Tyr} processing activity with various incubation times. The cleavage efficiency was calculated as follows: the quantity of (matured tRNA^{Tyr} + leader fragment)/the quantity of (pre-tRNA^{Tyr} + matured tRNA^{Tyr} + leader fragment), and the percentage was plotted against the incubation times.

2.5. FRET-based assay

FRET assays were principally performed as described previously [15], with some modifications [13]. Two fluorescence-labeled RNAs, Cy3-21R− (Cy3 – 5′ – ACUGCUAGAGAUUUUCCACAU-3′) and Cy5-21R+ (Cy5 – 5′ – AUGUGGAAAAUCUCUAGCAGU-3′), were obtained from Operon Biotechnologies (Tokyo). A nonfluorescence-labeled competitor RNA (21R−) with a sequence identical to Cy3-21R− was produced by *in vitro* transcription with T7 RNA polymerase using a corresponding synthetic DNA oligonucleotide as template. The resulting RNA was purified by ion-exchange column chromatography on a HiTrap DEAE Sepharose FF column, as described by Easton et al. [16]. We monitored FRET from the donor Cy3 to the acceptor Cy5 in 50 mM Tris–HCl (pH 7.5) containing 3 mM $MgCl_2$ and 1 mM DTT at 30 °C by measuring the fluorescence emission at 590 nm of Cy3 with excitation at 535 nm every 2 s using a fluorescence spectrophotometer (F-3010, Hitachi, Tokyo). In the first reaction (phase I), Cy3-21R− and Cy5-21R+ were annealed in a cell (1 mL). Annealing was started by mixing 300 μL of 100 nM Cy3-21R− with an equal volume of 100 nM Cy5-21R+ in the absence or presence of 200 μL of the protein (1 μM). The reaction was allowed to proceed for 1200 s. For the second reaction (phase II), 200 μL of 100 nM 21R− was added, the mixture was agitated vigorously, and measurements were continued for another 1200 s. The energy transfer efficiency (E) was calculated as follows: $E = 1 - F_{AD}/F_D$, where F_D and F_{AD} are fluorescence intensities of the donor (Cy3-21R−) in the absence and presence of the acceptor (Cy5-21R+), respectively [17]. Furthermore, the normalized energy transfer efficiency (NE) was calculated as $NE = E_t/E_{1200}$ in phase I and $NE = (E_t - E_{2400})/(E_{1200} - E_{2400})$, where E_t is the E at each time, and E_{1200} and E_{2400} are the values of E at 20 and 40 min, respectively.

3. Results

3.1. The pre-tRNA cleavage activity of the reconstituted particles

The crystal structure of *Pho*Pop5 is shown in Fig. 1A. It folds in a way that is topologically similar to the RNA recognition motif [10]. *Pho*Pop5 is, however, distinct from the typical RRM in that it has an insertion of α-helix (α2) between α1 and β2. Biochemical and structural data have shown that the loop between α1 and α2 is involved in dimerization of *Pho*Pop5 (Fig. 1B), which is required for pre-tRNA cleavage activity of the reconstituted particle [10].

In addition, *Pho*Pop5 has additional helices, α4 and α5, at the C-terminus (Fig. 1A and C), which pack against one face of the β-sheet that is most commonly used to interact with single-stranded RNA [18]. Furthermore, the electrostatic potential analysis indicates a large electropositive surface on the C-terminal helices [10], suggesting that the C-terminal helices are involved in the activation of *Pho*pRNA. To address this assumption, we prepared two mutants, Δ6C and Δ14C, in which the 6 and 14 C-terminal residues were deleted, respectively. The mutant proteins were purified in the same manner as described for wild-type *Pho*Pop5. The secondary structure of the two mutants was checked by examining the CD spectrum in the 200–250 nm region, reflecting backbone polypeptide chain conformations. Although the CD spectra of mutants in the short-wavelength region were slightly changed due to the truncation of helices, they were essentially the same as that of the wild-type *Pho*Pop5 (Supplementary Fig. S1). Therefore, the backbone conformation of the mutant proteins appeared to be practically the same as that of *Pho*Pop5.

We first carried out a time-course experiment (0–1 h) for the pre-tRNA cleavage activities of the reconstituted particles containing either wild-type *Pho*Pop5 or its mutants and assessed the contribution of the C-terminal helices to the pre-tRNA cleavage activity (Supplementary Fig. S2). On the basis of this result, the pre-tRNA cleavage efficiency was calculated as described in Section 2 (Fig. 2). The truncation of the 14 C-terminal residues significantly reduced the pre-tRNA cleavage activity; the reconstituted particle containing the mutant protein Δ14C exhibited 25% activity at 1 h compared with that containing wild-type *Pho*Pop5. In contrast, the removal of the 6 C-terminal residues had no influence on the enzymatic activity of the reconstituted particle, as shown in Fig. 2. This result suggested that the C-terminal helix α4 plays a crucial role in the activation of *Pho*pRNA for the pre-tRNA cleavage activity.

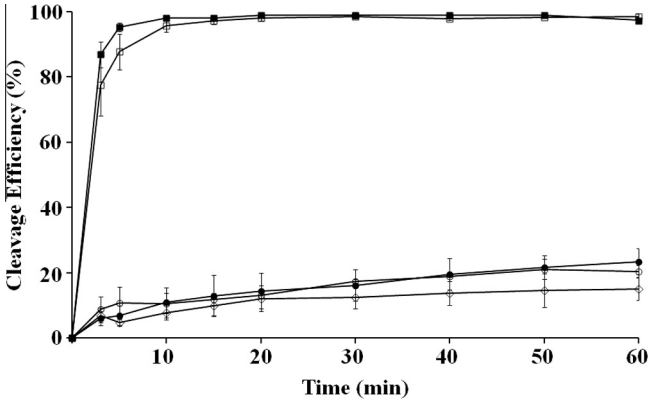

Fig. 2. The pre-tRNA cleavage activity of the *in vitro* reconstituted RNase P containing either *Pho*Pop5 or its mutants. Pre-tRNA cleavage activities of the reconstituted mixtures were assayed at 75 °C using *P. horikoshii* pre-tRNA^{Tyr}, as described in Section 2. The reaction volume was 200 μl and a small aliquot (10 μl) was withdrawn at the following time points: 10, 20, 30, 45, and 60 min. The reactions were stopped using a phenol extract. The cleavage products were resolved on 10% acrylamide/8 M urea/TBE gels and visualized by staining the gels in a 0.1% toluidine blue N solution. The individual bands were quantified using Multi Gauge V3.1 and the cleavage efficiency was calculated as (tRNA + 5′-leader fragment)/(pre-tRNA + tRNA + 5′-leader fragment) × 100. The experiments were carried out in triplicate, and the mean values are presented. The reconstituted particles with *Pho*Pop5 (■), Δ6C (□), Δ14C (●), ΔL43–48 (○), or without *Pho*Pop5 (◇).

In this study, we re-examined the pre-tRNA cleavage activity of the reconstituted particle containing ΔL43–48, in which Leu43-Glu48 at the loop between α1 and α2 were deleted, because

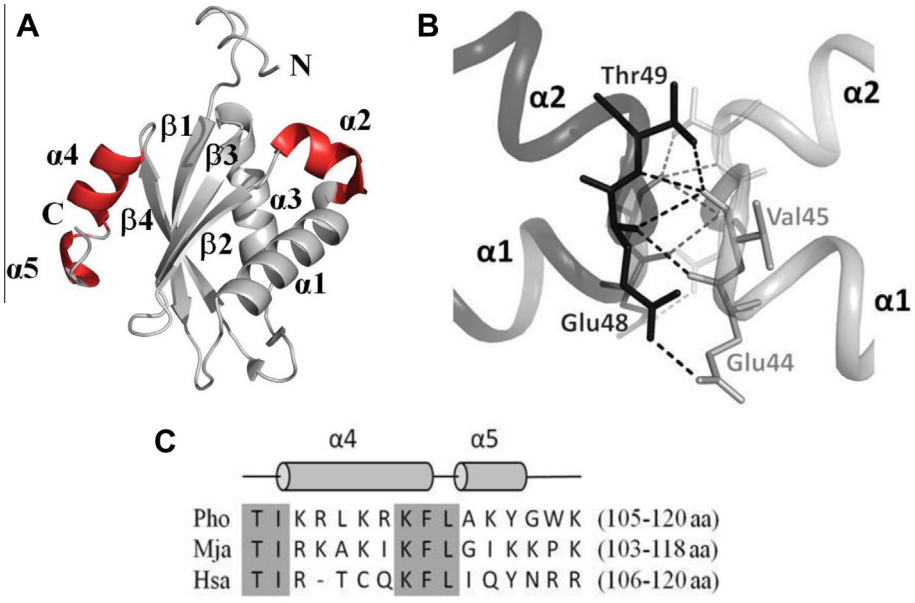

Fig. 1. The C-terminal helices of *Pho*Pop5. (A) Three-dimensional structure of *Pho*Pop5 (PDB accession code 2CZV) was drawn using Pymol (http://www.pymol.org). The secondary structures are labeled, and N and C termini are indicated. Extra-structural elements in the RRM in *Pho*Pop5 are highlighted in red. (B) A hydrogen bond network at the interface for the *Pho*Pop5 homodimer. The amino acid residues from Glu44 to Thr49 at the loop between α1 and α2 are involved in the interaction. (C) Sequence alignment of the C-terminal helices of the Pop5 family proteins. The three amino acid sequences of the Pop5 family proteins from *P. horikoshii* (Pho), *Methanococcus jannaschii* mj0494p (Mja), and *Homo sapiens* hPop5 (Hsa) were aligned. The C-terminal α-helices are indicated by bars. The amino acid residues highlighted in gray represent complete conservation among the three proteins. (For interpretation of the references to color in this figure legend, the reader is referred to the web version of this article.)

conditions for the pre-tRNA cleavage assay were slightly modified, as described recently [14]. The reconstituted particle containing ΔL43–48, as reported previously [10], had virtually reduced pre-tRNA cleavage activity, as shown in Fig. 2. Since the reconstituted particles containing Δ14C or ΔL43–48 had the cleavage efficiencies comparable to that without *Pho*Pop5 (Fig. 2), these results indicated that extra-structural elements, α2 and α4, in the RRM in *Pho*Pop5 play an essential role in the activation of *Pho*pRNA.

3.2. FRET-based analysis

Our recent analysis by FRET using oligonucleotides indicates that *Pho*Pop5 is capable of promoting AN and SD [13], and it is thus speculated that *Pho*Pop5 assists *Pho*pRNA in attaining a functionally active conformation, probably by accelerating AN and SD. Next, we tested whether or not Δ6C, Δ14C, and ΔL43–48 retain the ability to enhance AN and SD using FRET-based analysis, as described in Section 2. In the presence of either ΔL43–48 or Δ6C, their FRET efficiencies were strongly increased (Fig. 3). When unlabeled RNA (21R−) was added, ΔL43–48 and Δ6C decreased the FRET efficiency between Cy3 and Cy5 linked to the complementary RNA strands (Fig. 3). This result indicated that ΔL43–48 and Δ6C retain the ability to accelerate AN and SD. Interestingly, ΔL43–48 appeared to promote AN and SD more strongly than wild-type *Pho*Pop5. This finding suggests that the dimerization through the loop between α1 and α2 may suppress the acceleration of AN and SD. In contrast, Δ14C showed a FRET curve similar to those of Cy3 and Cy5 linked to the complementary RNA strands in the absence of protein, indicating that elimination of the 14 C-terminal amino acids abolished the ability to enhance SD (Fig. 3). Collectively, the present FRET-based assay indicated that the C-terminal helix α4 is strongly involved in the acceleration of not only AN but also SD.

3.3. Essential amino acids for the activation of PhopRNA

For further examination of the amino acids in α4 that are essential for the *Pho*Pop5 activity, amino acids at positions 109–114 were individually replaced with Ala (Fig. 1C). The mutant proteins were purified in the same manner as described for wild-type *Pho*Pop5 and characterized again by the reconstitution experiment. The reconstituted particles containing mutants K107A, K112A, F113A, and L114A, in which Lys107, Lys112, Phe113, and Leu114 were individually replaced with Ala, respectively, exhibited moderately reduced pre-tRNA cleavage activities (Fig. 4A), whereas the other mutations had little influence on the activity. This result suggested that basic amino acids, Lys107 and Lys112, and hydrophobic residues, Phe113 and Leu114, function cooperatively in the activation of *Pho*pRNA. Examination of the crystal structure revealed that side chains of Lys107 and Lys112 extend toward the protein's surface, while those of Phe113 and Leu114 extend toward the β-sheet (Fig. 4B). Hence, Lys107 and Lys112 are involved in interaction with *Pho*pRNA, and hydrophobic residues Phe113 and Leu114 are responsible for stabilizing an appropriate orientation of the helix α4 by hydrophobic interaction with the β-sheet.

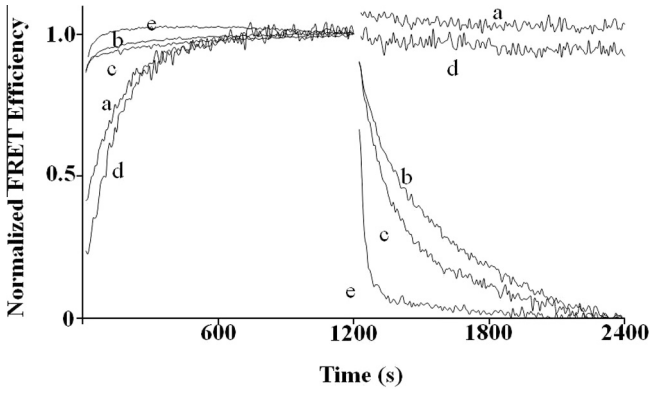

Fig. 3. FRET-based assay for RNA-binding properties of *Pho*Pop5 or its mutants. Fluorescence spectrophotometric analysis of two complementary RNAs (Cy5-21R+ and Cy3-21R−) in the absence or presence of the proteins. The energy transfer efficiency (E) was calculated as follows. $E = 1\text{-}F_{DA}/F_D$, where F_D and F_{AD} are relative fluorescence intensities of the donor (Cy3-21R−) in the absence and presence of the acceptor (Cy5-21R), respectively [16]. (a) Cy-21R+ and Cy-21R− with no protein; (b) Cy5-21R+ and Cy3-21R− with *Pho*Pop5; (c) Cy5-21R+ and Cy3-21R− with Δ6C; (d) Cy5-21R+ and Cy3-21R− with Δ14C; (e) Cy5-21R+ and Cy3-21R− with ΔL43–48.

4. Discussion

Rajkowitsch et al. described that RNA-binding proteins can be grouped into four classes on the basis of their mode of action [19]. The first group includes proteins that bind non-specifically to RNA and resolve kinetically trapped, misfolded conformers: these proteins are referred to as RNA chaperones. The second group includes proteins that accelerate annealing of complementary RNAs: these proteins are termed RNA annealers. The third and fourth groups include RNA helicases and specific RNA-binding proteins including the *E. coli* ribosomal protein L7/L12, respectively. Recently, FRET-based assays indicated that *Pho*Pop5, *Pho*Rpp21, *Pho*Rpp29, and *Pho*Rpp30 have the ability to promote AN and SD [13]; that is, the four proteins are classified into RNA chaperones and RNA annealers. This finding has led us to the speculation that they assist *Pho*pRNA in attaining a functionally active conformation by serving as RNA chaperones and RNA annealers. The FRET analysis was, however, carried out using non-specific oligonucleotides under binding conditions distinct from those used for pre-tRNA cleavage assay. Therefore, we could not correlate the RNA chaperone and annealer activities with the activation of *Pho*pRNA by the four proteins. However, the present analysis indicated that the C-terminal truncation influenced not only the pre-tRNA cleavage activity but also the promoting activity of AN and SD. Therefore, it is highly likely that the C-terminal helix α4 in *Pho*Pop5 activates *Pho*pRNA by serving as an RNA chaperone and RNA annealer.

*Pho*Pop5 folds into the RNA recognition motif (RRM), which is by far the most abundant type of eukaryotic RNA-binding motif. The RRM is approximately 90 amino acids long with a typical β1α1β2β3α2β4 topology that forms a four-stranded β-sheet packed against two α-helices [18]. Most commonly, the RRM specifically recognizes both single-stranded and highly structured RNAs, and two highly conserved amino acid sequences (RNP1 and RNP2) have been identified as binding sites in the central strands of an antiparallel β-sheet. Atypical features of *Pho*Pop5 are the presence of an α-helix (α2) between α1 and β1; the absence of the consensus RNP1 and RPN2 sequences on the β3 and β1 strands, respectively; and the C-terminal helices α4 and α5, which pack against one face of the β-sheet [10]. Biochemical and structural data revealed that the loop between α1 and α2 is involved in the dimerization of *Pho*Pop5, which is required for the activation of *Pho*pRNA. Probably, the dimerization may help in achieving higher affinity and specificity to *Pho*pRNA for *Pho*Pop5. The present study indicates that the positively charged residues, Lys107 and Lys112, on the C-terminal helix α4 are involved in the activation of *Pho*pRNA, and that hydrophobic residues Phe113 and Leu114 are involved in stabilizing an appropriate orientation of the helix α4 by hydrophobic interaction with the β-sheet. Hence, extra-structural elements, α2 and α4, in the RRM in *Pho*Pop5 play a crucial role in the activation of *Pho*pRNA.

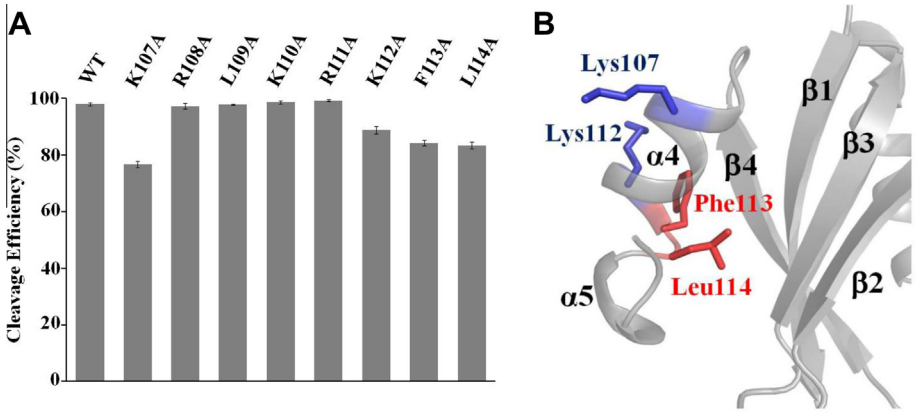

Fig. 4. The pre-tRNA cleavage activity of the *in vitro* reconstituted RNase P containing either *Pho*Pop5 or its Ala mutants. (A) The pre-tRNA cleavage activities of the reconstituted mixtures containing *Pho*Pop5 or its Ala mutants were assayed, as described in Fig. 2. The pre-tRNA cleavage efficiencies by the reconstituted particles containing *Pho*Pop5 or its Ala mutants at 10 min are expressed. The experiments were carried out in triplicate. (B) Side chains of amino acid residues located at α4. The side chains of basic residues, Lys107 and Lys112, shown in blue extend toward the protein's surface, while hydrophobic residues, Phe113 and Leu114, in red extend toward the β-sheet. (For interpretation of the references to color in this figure legend, the reader is referred to the web version of this article.)

Similar findings have been reported for several RRM proteins with non-canonical extensions, such as the *Saccharomyces cerevisiae* pre-messenger splicing factor Prp24 [20], La proteins [21], and the C-terminal domain of La family protein p65 [22]. Although biochemical data have become available for RRM proteins exhibiting AN- and SD-promoting activity, the molecular basis for RNA chaperones and annealers has remained unclear. A structural study of *Pho*Pop5 in complex with *Pho*pRNA will definitely provide a molecular basis for understanding how RNA chaperones and annealers can enhance the folding of their RNA targets.

Acknowledgments

We are grateful to Prof. S. Yamashita (Kyushu University) and Dr. M. Teramoto (National Institute of Environmental Health Sciences at Durham in USA) for their useful suggestions. This work was supported in part by a Grant-in-aid for scientific research from the Ministry of Education, Culture, Sports, Science, and Technology of Japan (No. 22380062 to M.K.).

Appendix A. Supplementary data

Supplementary data associated with this article can be found, in the online version, at http://dx.doi.org/10.1016/j.bbrc.2013.09.140.

References

[1] L.A. Kirsebom, S. Trobro, RNase P RNA-mediated cleavage, IUBMB Life 61 (2009) 189–200.
[2] O. Esakova, A.S. Krasilnikov, Of proteins and RNA: the RNase P/MRP family, RNA 16 (2010) 1725–1747.
[3] C. Guerrier-Takada, K. Gardiner, T. Marsh, N. Pace, S. Altman, The RNA moiety of ribonuclease P is the catalytic subunit of the enzyme, Cell 35 (1983) 849–857.
[4] N. Jarrous, V. Gopalan, Archaeal/Eukaryal RNase P: subunits, functions and RNA diversification, Nucleic Acids Res. 38 (2010) 7885–7894.
[5] J.A. Pannucci, E.S. Haas, T.A. Hall, J.K. Harris, J.W. Brown, RNase P RNAs from some archaea are catalytically active, Proc. Natl. Acad. Sci. USA 96 (1999) 7803–7808.
[6] E. Kikovska, S.G. Svard, L.A. Kirsebom, Eukaryotic RNase P RNA mediates cleavage in the absence of protein, Proc. Natl. Acad. Sci. USA 104 (2007) 2062–2067.
[7] Y. Kouzuma, M. Mizoguchi, H. Takagi, H. Fukuhara, M. Tsukamoto, T. Numata, M. Kimura, Reconstitution of archaeal ribonuclease P from RNA and four protein components, Biochem. Biophys. Res. Commun. 306 (2003) 666–673.
[8] H. Fukuhara, M. Kifusa, M. Watanabe, A. Terada, T. Honda, T. Numata, Y. Kakuta, M. Kimura, A fifth protein subunit Ph1496p elevates the optimum temperature for ribonuclease activity from *Pyrococcus horikoshii* OT3, Biochem. Biophys. Res. Commun. 343 (2006) 956–964.
[9] A. Terada, T. Honda, H. Fukuhara, K. Hada, M. Kimura, Characterization of the archaeal ribonuclease P proteins from *Pyrococcus horikoshii* OT3, J. Biochem. 140 (2006) 293–298.
[10] S. Kawano, T. Nakashima, Y. Kakuta, I. Tanaka, M. Kimura, Crystal structure of protein Ph1481p in complex with protein Ph1877p of archaeal RNase P from *Pyrococcus horikoshii* OT3: implication of dimer formation of the holoenzyme, J. Mol. Biol. 357 (2006) 583–591.
[11] T. Honda, Y. Kakuta, K. Kimura, J. Saho, M. Kimura, Structure of an archaeal homolog of the human complex Rpp21–Rpp29 that is a key core component for the assembly of active ribonuclease P, J. Mol. Biol. 384 (2008) 652–662.
[12] T. Honda, T. Hara, J. Nan, X. Zhang, M. Kimura, Archaeal homologs of human RNase P protein pairs Pop5 with Rpp30 and Rpp21 with Rpp29 work on distinct functional domains of the RNA subunit, Biosci. Biotechnol. Biochem. 74 (2010) 266–273.
[13] M. Ishihara, E. Nishimoto, S. Yamashita, Y. Kakuta, M. Kimura, A distinct binding mode of archaeal ribonuclease P proteins to RNA, Biosci. Biotechnol. Biochem. 76 (2012) 2335–2337.
[14] T. Ueda, H. Yamaguchi, M. Miyanoshita, T. Nakashima, Y. Kakuta, M. Kimura, Characterization of the peripheral structures of archaeal RNase P RNA from *Pyrococcus horikoshii* OT3, J. Biochem. (2013) in press (JB-13-09-0241).
[15] L. Rajkowitsch, R. Schroeder, Coupling RNA annealing and strand displacement: a FRET-based microplate reader assay for RNA chaperone activity, Biotechniques 43 (2007) 304–310.
[16] L.E. Easton, Y. Shibata, P.J. Lukavsky, Rapid, nondenaturing RNA purification using weak anion-exchange fast performance liquid chromatography, RNA 16 (2010) 647–653.
[17] J.R. Lakowicz, Principles of Fluorescence Spectroscopy, third ed., Springer Science + Business Media, New York, 2006.
[18] A. Clery, M. Blatter, F.H.T. Allain, RNA recognition motifs: boring? Not quite, Curr. Opin. Struct. Biol. 18 (2008) 290–298.
[19] L. Rajkowitsch, D. Chen, S. Stampfl, K. Semrad, C. Waldsich, O. Mayer, M.F. Jantsch, R. Konrat, U. Blasi, R. Schroeder, RNA chaperones, RNA annealers and RNA helicases, RNA Biol. 4 (2007) 118–130.
[20] S. Martin-Tumasz, A.C. Richie, L.J. Clos II, D.A. Brow, S.E. Butcher, A novel occluded RNA recognition motif in Prp24 unwinds the U6 RNA internal stem loop, Nucleic Acids Res. 39 (2011) (2011) 7837–7847.
[21] A.R. Naeeni, M.R. Conte, M.A. Bayfield, RNA chaperone activity of human La protein is mediated by variant RNA recognition motif, J. Biol. Chem. 287 (2012) 5472–5482.
[22] M. Singh, Z. Wang, B.K. Koo, A. Patel, D. Cascio, K. Collins, J. Feigon, Structural basis for telomerase RNA recognition and RNP assembly by the holoenzyme La family protein p65, Mol. Cell 47 (2012) 16–26.